Identification of Prompt Proton Emission in $N = Z - 1$ ^{61}Ga: Isospin Symmetry at the Limit of Nuclear Binding

Y. Hrabar,[1,*] P. Golubev,[1] D. Rudolph,[1] L. G. Sarmiento,[1] C. Müller-Gatermann,[2] W. Reviol,[2] D. Seweryniak,[2] J. Wu,[2,†] H. M. Albers,[3] J. T. Anderson,[2] M. A. Bentley,[4] B. G. Carlsson,[1] M. P. Carpenter,[2] C. J. Chiara,[5] P. A. Copp,[2,‡] D. M. Cox,[1] J. Ekman,[6] C. Fahlander,[1] U. Forsberg,[1,§] T. Huang,[2,‖] A. Idini,[1] H. Jayatissa,[2,‡] T. Lauritsen,[2] X. Pereira-Lopez,[4,¶] S. Stolze,[2] S. Uthayakumaar,[4,**] and G. L. Wilson[2,7,††]

[1]*Department of Physics, Lund University, SE-22100 Lund, Sweden*
[2]*Physics Division, Argonne National Laboratory, Lemont, Illinois 60439, USA*
[3]*GSI Helmholtzzentrum für Schwerionenforschung, DE-64291 Darmstadt, Germany*
[4]*School of Physics, Engineering and Technology, University of York, Heslington, York, YO10 5DD, United Kingdom*
[5]*U.S. Army Combat Capabilities Development Command Army Research Laboratory, Adelphi, Maryland 20783, USA*
[6]*Department of Materials Science and Applied Mathematics, Malmö University, SE-20506 Malmö, Sweden*
[7]*Department of Physics and Astronomy, Louisiana State University, Baton Rouge, Louisiana 70803, USA*

(Received 2 September 2024; revised 23 September 2025; accepted 7 November 2025; published 25 November 2025)

Excited states in the proton drip line nucleus ^{61}Ga were populated via the fusion-evaporation reaction ^{24}Mg(^{40}Ca, $p2n$)^{61}Ga. The experimental setup at Argonne National Laboratory comprised a novel combination of the Gammasphere array with two CD-shaped double-sided Si-strip detectors inside the Microball CsI(Tl) charged-particle detection array, as well as the Neutron-Shell liquid scintillators and the Fragment Mass Analyzer. Owing to the setup's unprecedented in-beam proton spectroscopy and tracking capabilities, a coincidence between a 957.6(5)-keV γ ray and a 1.876(24)-MeV proton line was observed, which identifies the quasibound proton $\pi g_{9/2}$ single-particle state in ^{61}Ga at $E_x = 2150(34)$ keV. This probes isospin symmetry at the limit of nuclear binding by providing a unique challenge for the shell-model interpretation of mirror nuclei beyond doubly magic ^{56}Ni.

DOI: 10.1103/kwm2-9bmd

A central topic in contemporary nuclear-structure physics is the investigation of exotic atomic nuclei far from the line of β stability. Experimentally, one way of addressing fundamental questions in the field is to study the outskirts of the nuclear landscape by performing detailed spectroscopy of ground or low-lying excited states in nuclei at or beyond the drip lines. One region of interest on the nuclide chart is $N \approx Z$ nuclei just above the self-conjugate, doubly magic nucleus ^{56}Ni. Notably, odd-Z, $N < Z$ nuclei with mass $A \gtrsim 60$ are weakly if at all bound against proton emission. Therefore, exploring the laboratory of their excited states, and comparing the results with isobaric analog states of their well-bound even-Z "mirror partners," provides information on isospin symmetry breaking at or beyond the proton drip line. The underlying nuclear-structure question concerns the continued applicability of shell-model-based prescriptions of subtle isospin-breaking phenomena [1,2] in case quasibound states are involved. Such knowledge is also crucial for elucidating the rapid-proton capture process in nuclear astrophysics (see, e.g., Refs. [3,4]), because the nuclear properties of these exotic nuclei impact modeling rapid-proton capture pathways, thereby influencing the synthesis of heavier elements in stellar environments.

The study of excited-state energy differences of analog states in mirror nuclei has been extremely successful over the years, in particular, in the lower fp-shell region between ^{40}Ca and ^{56}Ni [1,2]. Only a few low-lying excited

*Contact author: yuliia.hrabar@fysik.lu.se
†Present address: Brookhaven National Laboratory, Brookhaven, USA.
‡Present address: Physics Division, Los Alamos National Laboratory, Los Alamos, USA.
§Present address: Cyclife Sweden AB, Nyköping, Sweden.
‖Present address: Institute of Modern Physics, Chinese Academy of Sciences, Lanzhou 730000, China.
¶Present address: Center for Exotic Nuclear Studies, Institute for Basic Science, Daejeon, Republic of Korea.
**Present address: Facility for Rare Isotope Beams, Michigan State University, East Lansing, USA.
††Present address: United Kingdom Atomic Energy Authority, Abingdon, United Kingdom.

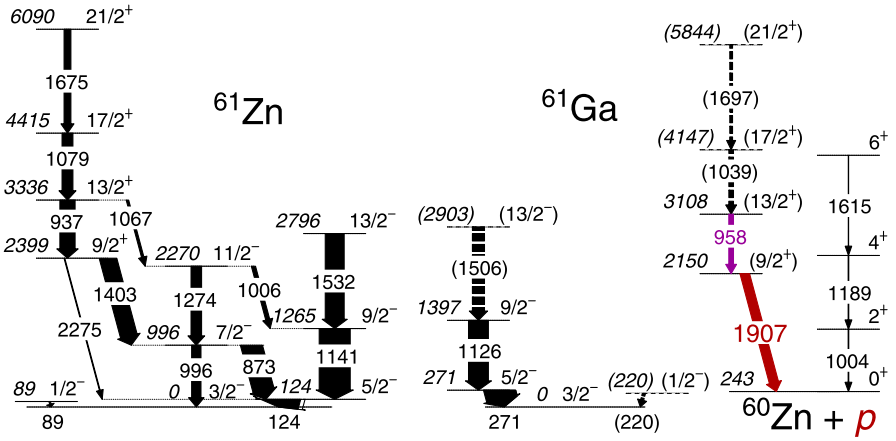

FIG. 1. Proposed level scheme for ^{61}Ga (right) [7] and relevant parts of the level schemes of the mirror nucleus ^{61}Zn (left) [15] and of ^{60}Zn (rightmost) [17]. The newly identified proton emission [$E_p = 1.876(24)$ MeV, $Q_p = 1.907(24)$ MeV] from the 2150-keV $(9/2^+)$ state in ^{61}Ga is marked in red. The coincident 958-keV γ ray feeding the 2150-keV state is marked magenta. Energy labels are in keV and relative to the ground state of ^{61}Ga [18–20]. Tentative transitions and levels are dashed. The widths of the arrows correspond to relative intensities of the transitions.

states in ^{57}Cu had been known [5], while an increasing amount of information has been collected over the past few years for heavier $N < Z$ nuclei in the upper fp shell. This concerns isotope-selective γ-ray spectroscopy following either fusion-evaporation reactions (see, e.g., ^{59}Zn, ^{61}Ga, ^{62}Ge, or ^{67}Se [6–9]) or, more recently, by means of high-energy nucleon-removal reactions (see, e.g., ^{56,58}Zn, ^{62}Ge, or ^{79}Zr [3,9–11]).

However, besides the identification of a few states in ^{57}Cu [5] and a single state in ^{65}As [12], the early study on ^{61}Ga [7] remained the only one for an odd-Z $N < Z$ isotope in the region. An explanation for the lack of experimental information on those nuclei lies in their intertwined challenge and interest: Weak nuclear binding requires comprehensive experiments including dedicated detection systems to be sensitive to fast proton emission in direct competition to γ-ray emission.

This Letter reports on the identification of a proton-emitting state at $E_x = 2150(34)$ keV in the weakly bound $N < Z$, $T_z = -1/2$ nucleus ^{61}Ga; T_z is the isospin-projection quantum number. This state is interpreted as the proton $\pi g_{9/2}$ single-particle state according to the decay schemes of the $A = 61$, $T_z = \pm 1/2$ mirror nuclei ^{61}Ga and ^{61}Zn [13–15] shown in Fig. 1. The observation of this state opens up the crucial questions of how well isospin symmetry holds at the very limit of weak nuclear binding (see, e.g., Ref. [16]) and how well the best nuclear models can reproduce the observed deviations under those conditions. Moreover, in this Letter, we present the first observation, in a mirror pair, of a sequence of isobaric analog states built upon a single-particle state which, in one of the two nuclei, is a proton emitter.

The experiment was conducted at the ATLAS facility at Argonne National Laboratory (ANL), USA. Excited states in ^{61}Ga were populated by the fusion-evaporation reaction $^{40}\mathrm{Ca} + {}^{24}\mathrm{Mg} \rightarrow {}^{64}\mathrm{Ge}^*$, following the evaporation of one proton and two neutrons ($p2n$ channel). The $^{40}\mathrm{Ca}^{19+}$ ion beam was accelerated to 106 MeV with an average intensity of about 60 enA. The self-supporting ^{24}Mg target foil had a thickness of 0.43 mg/cm^2 and 99.92% isotopic enrichment.

The focus of the experiment was state-of-the-art in-beam proton-γ coincidence spectroscopy based on an advanced approach for charged-particle detection. Two CD-shaped double-sided Si-strip detectors (DSSDs) [21–23] and the Microball CsI(Tl) array [24] were placed inside a target chamber, surrounded by Gammasphere [25] and Neutron-Shell [26] arrays. Gammasphere comprised 71 Ge-detector modules for high-resolution γ-ray detection. The heavymet collimators of the Compton suppressors of the Gammasphere array were removed to measure γ-ray multiplicity (k) and sum energy (H) of all γ rays detected in Gammasphere, its suppressors, and the neutron detectors [23]. This option is known to allow for improved reaction-channel selection [27]. The neutron detectors replaced the 32 most forward Ge-detector modules in the beam direction. For neutron-γ separation in these detectors and proton-α separation in Microball CsI(Tl) elements, standard pulse-shape discrimination was used. This was combined with time-of-flight information with respect to the pulsed beam from ATLAS. After particle evaporation and prompt γ-ray emission, reaction products recoiling from the target could enter the Fragment Mass Analyzer (FMA) [28]. Data from the FMA were utilized for the determination of the recoil's mass-over-charge ratio A/q. An ionization chamber (IC) located at the FMA's focal plane collected information on the recoil's atomic number. For further details, see Supplemental Material [21] and Refs. [22,23].

The novel combination of DSSDs and Microball [21–23], acting as a highly pixelated ΔE-(ΔE-)E telescope system, enabled unprecedented proton tracking, light charged-particle identification, and optimized energy resolution, all while maintaining high detection efficiency [29]. The tracking capabilities of the DSSD system were exploited to determine the original beam-spot position on the target foil as a function of experiment time (beam tune) [30]. As the beam-spot displacement from the centered position was similar in size to a single DSSD pixel, it was included in the reconstruction of the recoil vector and final center-of-mass proton energies [21].

Data analysis involved energy calibration and time alignment for all channels across all detector systems, followed by particle identification in each detector system [22,23,31,32]. In addition to γ rays detected in the Ge detectors, the following information became available for each event: number of detected protons, deuterons, α particles, and neutrons, total γ multiplicity k, total γ energy H, total particle energy P, and, if detected, mass number A and energy loss in the IC of the recoil. For each particle, energies as well as θ and ϕ angles in the laboratory frame were used to reconstruct event-specific recoil vectors that accounted for particle evaporation. Doppler corrections were applied to obtain γ-ray and proton energies in the center-of-mass frame. Prompt proton energies from ^{61}Ga candidates were corrected for energy loss in the Ta absorber foils [33]. The entire procedure was validated with Geant4 simulations [34–36] to account for detector geometry and recoil kinematics, minimizing systematic uncertainties, as detailed in Refs. [21–23]. These parameters were combined in various ways to analyze specific reaction channels, in particular, prompt proton emission from excited states in ^{61}Ga ($p2n$ channel) into the ground state of ^{60}Zn (see Fig. 1).

The vast majority of protons observed during the experiment originated from evaporation of the main reaction channels ^{58}Ni ($\alpha 2p$) [37], ^{61}Cu ($3p$) [38], or ^{61}Zn ($2pn$) [14,15]. Therefore, in order to improve the signal-to-background ratio, very strict selection conditions had to be applied to identify proton-line candidates from ^{61}Ga. Technical difficulties during data recording [39] caused reduced statistics in detected neutrons and Z separation for the nuclei of interest in the IC [23]. Nevertheless, owing redundancies in the detection scheme, the following conditions were imposed to search for proton-γ coincidences stemming from ^{61}Ga: (i) mass $A = 60$ recoils in the FMA, (ii) total γ-ray multiplicity $k > 3$, (iii) coincidence time $\Delta t < 200$ ns between a proton candidate and a γ ray, (iv) total number of protons detected $N_p = 1$ or 2, and (v) at least one of the protons had to be identified solely in the first DSSD. With an expected $Q_p \approx 2.0$–2.5 MeV, laboratory-frame proton energies after the Ta absorbers are $E_{p,\mathrm{lab}} < 5$ MeV; i.e., such protons deposit all remaining energy in that DSSD [21].

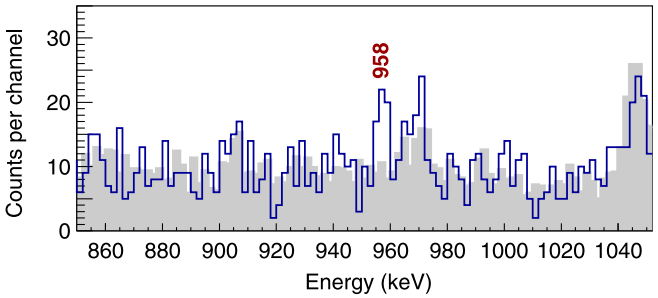

FIG. 2. Measured γ-ray energy spectrum (dark blue) in coincidence with $E_p = [1.75, 2.05]$ MeV. The background is depicted in gray. The 958-keV transition of interest is labeled in dark red with its energy in keV. The binning is 2 keV per channel. See the text for details on reaction-selection criteria.

Under those conditions, an E_p-E_γ correlation matrix was searched for γ-ray coincidences with $Q_p \approx 2.0$-MeV protons [7]. The result is shown in Fig. 2. The γ-ray spectrum (dark blue) reveals a peak at 957.6(5) keV. This is a previously unknown γ ray and close in energy to the 937-keV mirror transition in ^{61}Zn [14]. The statistical significance of counts above background of the peak is 4.3σ according to the standard Poisson-statistics particle-physics test for the discovery probability value. Furthermore, the peak has a width and shape compliant with its energy.

Followed by the discovery of the 958-keV γ-ray transition, a coincidence with this transition in the E_p-E_γ correlation matrix gives rise to the proton energy spectrum in Fig. 3 (dark blue). The spectrum shows a 1.876(24)-MeV proton line in the E_p range of interest on top of the normalized background spectrum (black and gray), which is in coincidence with any $E_\gamma = [900, 1100]$ keV. The full width at half maximum of the peak is 0.19(5) MeV and in line with expectations [21,29], in contrast to other (statistically nonsignificant) peaklike structures at higher proton energies in Fig. 3. Notably, the observed proton line disappears when changing the condition $N_p = 1, 2$ to $N_p \geq 3$ (corresponding to final residues ^{60}Cu or ^{60}Ni) [21], and the production cross section of ^{61}Ge ($3n$ channel) is essentially zero at the beam energy used (residue ^{60}Ga). It is also worth stressing that the peak structure improves using the tracking corrections of varying beam-spot positions [21–23].

Since a coincidence relationship with the yrast ground-state transition in ^{60}Zn is absent, the proton line at $E_p = 1.876(24)$ MeV [$Q_p = 1.907(24)$ MeV] is associated with the decay of the proton $\pi g_{9/2}$ single-particle state in ^{61}Ga into the ground state of ^{60}Zn. The similarity in γ-ray energy with ^{61}Zn of the γ ray feeding the proton-emitting state (cf. Fig. 1) clearly supports this assignment. The ground state of ^{61}Ga is bound by 243(23) keV [18–20]; i.e., the proton-emitting $(9/2^+)$ state is found at

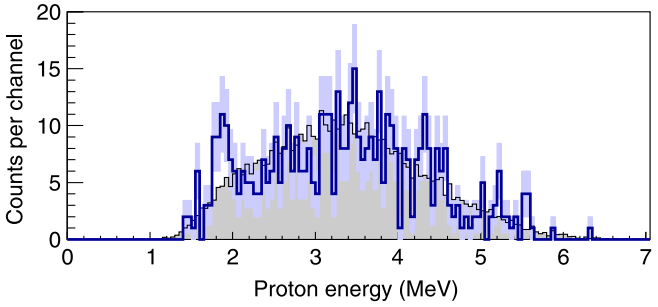

FIG. 3. Center-of-mass proton energy spectrum in coincidence with a 958-keV γ ray associated with ^{61}Ga according to selection criteria specified in the text. The spectrum is shown in dark blue together with statistical uncertainties (shaded light blue) plotted on top of a normalized background spectrum (black and gray). The binning is 50 keV per channel.

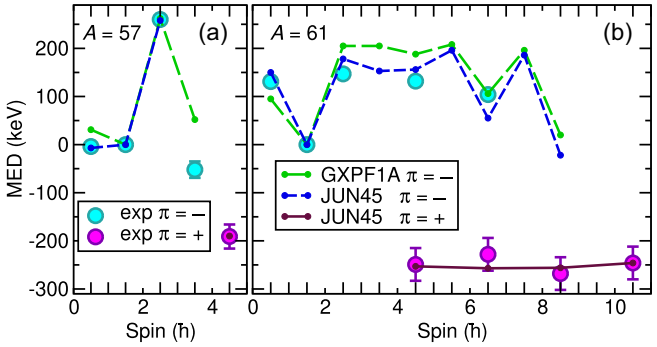

FIG. 4. Experimental and calculated MED for the $T_z \pm 1/2$, $A = 57$ nuclei ^{57}Cu and ^{57}Ni [4,5,40] [(a)] and the $A = 61$ mirror pair ^{61}Ga and ^{61}Zn [7,13–15] [(b)]. Experimental data are shown as filled turquoise ($\pi = -$) and magenta ($\pi = +$) circles, respectively. Calculations for negative-parity states are represented by (long-)dashed lines (GXPF1A, green; and JUN45, blue), while solid lines correspond to the prediction for MED values of positive-parity states (JUN45, maroon).

$E_x(^{61}\mathrm{Ga}) = 2150(34)$ keV. On top of that state, the 958-keV γ ray as well as tentative 1039- and 1697-keV γ-ray transitions (see Supplemental Material [21]) are proposed to form the positive-parity $(13/2^+)$, $(17/2^+)$, and $(21/2^+)$ yrast sequence, to be compared with the 937-, 1079-, and 1675-keV cascade known to feed the neutron $\nu g_{9/2}$ $9/2^+$ state at $E_x(^{61}\mathrm{Zn}) = 2399$ keV [14,15].

Finally, a $\gamma\gamma$ matrix selected by mass $A = 61$ was studied to possibly extend the known negative-parity decay scheme of ^{61}Ga [7]. Only the previously reported γ rays and coincidences could be confirmed. The results are summarized in the decay scheme of ^{61}Ga in Fig. 1 together with the relevant part of the decay scheme of the mirror nucleus ^{61}Zn.

The mirror energy difference (MED) of the $T_z = \pm 1/2$, $A = 61$ $9/2^+$ states is MED $= -249(34)$ keV, based on the weighted mean of evaluated mass and recent mass measurements of ^{61}Ga [18–20]. The $A = 61$ MED is even larger in size than MED $= -191(25)$ keV for the corresponding $9/2^+$ states in the $T_z = \pm 1/2$, $A = 57$ mirror pair [5,40]. Notably, the $9/2^+$ states in both ^{57}Cu and ^{61}Ga are proton unbound.

Experimental and predicted MED for the $A = 57$ and 61 mirror nuclei are presented in Fig. 4. For the predictions, given the proximity to doubly magic ^{56}Ni, shell-model calculations were performed with the code Antoine [41,42]. Two common interactions were explored. First, for the negative-parity states, GXPF1A [43] covering the full fp space was used. It was modified to include isospin-breaking terms according to [2,44,45], i.e., Coulomb multipole matrix elements, V_{CM}, of proton-proton two-body matrix-elements (TBME), $V_{B:2} = +100$ keV to the $f_{7/2}$ proton-proton $J = 2$ TBME [45], and modifications of single-particle energies (SPE) due to electromagnetic spin-orbit contributions, $V_{C\ell s}$, as well as radial effects, V_{Cr}. The latter relates to differences in proton minus neutron occupation numbers between the excited and ground states [2]. The calculations were limited to $t = 6$ ($A = 57$) and $t = 5$ ($A = 61$) excitations across the shell gaps at ^{56}Ni, respectively. Second, JUN45 [46] was used to allow for the description of positive- and negative-parity states in unrestricted calculations in the $f_{5/2}pg_{9/2}$ space [47]. Furthermore, for JUN45 an isospin-breaking interaction file had to be developed [48], using calculated contributions for V_{CM} and $V_{C\ell s}$ [21]. From the calculated $V_{C\ell s}$ and MED of observed SPE states in $A = 41$ and $A = 57$ mirror nuclei, $V_{\mathrm{Cr}}(p_{3/2}) = -300$ keV, $V_{\mathrm{Cr}}(p_{1/2}) = -410$ keV, $V_{\mathrm{Cr}}(f_{5/2}) = -220$ keV, and $V_{\mathrm{Cr}}(g_{9/2}) = -380$ keV, relative to the $f_{7/2}$ proton SPE, were extracted.

With the isospin-breaking JUN45 interaction fixed at $A = 57$ (see above and [21]), its prediction for the ^{61}Ga-^{61}Zn pair is trustworthy. As illustrated in Fig. 4, the calculations reproduce both the large positive values (MED $\approx +150$ keV) of the negative-parity states [7] as well as the large negative values (MED ≈ -250 keV) of the positive-parity states. The latter is ≈ -60 keV different from the corresponding $A = 57$ $\pi g_{9/2}$ single-particle value. About half of the large negative MED stems from the electromagnetic spin-orbit effect [1,2,49]: Assuming pure single-particle $p_{3/2}$ ground states and $g_{9/2}$ excited states, MED $= -110$ keV follows. Furthermore, for the negative-parity states, the level of agreement is similar for the interactions GXPF1A and JUN45.

Although there is very good agreement between observed and predicted MED (cf. Fig. 4), a few words of context are in order. Unlike $N \approx Z$ nuclei between ^{40}Ca and ^{56}Ni, for which shell-model parametrizations allow for detailed comparisons with experiment [1,2,50], predictions for near-spherical $N \approx Z$, $A \approx 60$ nuclei appear overall less reliable (see, e.g., the assessment of low-spin negative-parity states in ^{63}Ga [51]). While the former descriptions are

dominated by rather well-isolated and well-understood $f_{7/2}$ TBME, similar in all commonly used shell-model interactions in the respective mass region, the latter are subject to (varying) details of SPE and TBME related to the close-lying upper-fp shell orbitals $p_{3/2}$, $f_{5/2}$, and $p_{1/2}$. In combination with the $V_{C\ell s}$ term, quite different for protons and neutrons occupying $p_{3/2}$ ($j = \ell + s$) or $f_{5/2}$ ($j = \ell - s$) orbitals, this can lead to variations in observed, and predicted, MED in the mass region of the current study. Given these issues, the agreement between the experimental and calculated MED is excellent, for states of both parities in the $A = 61$ pair. This is especially remarkable for the MED for the two $9/2^+$ states, given that, in ^{57}Cu and ^{61}Ga, they are proton unbound, which one would expect to have consequences on the radial contributions V_{Cr}. For the newly observed sequence of states built upon the unbound $9/2^+$ proton emitter, the near-constant MED (and near-zero MED relative to the $9/2^+$ band-head state) suggests a stable configuration with increasing J, characteristic of a sequence of rotational states built upon a deformed intruder state.

The $\pi g_{9/2}$ ($\nu g_{9/2}$) single-particle character of the $9/2^+$ state in ^{61}Ga (^{61}Zn) is substantiated by predicted partitions of $\approx 45\%\ \pi(g_{9/2}) \times \pi(fp)^2_0 \times \nu(fp)^2_0$ configurations and an occupation number $n_{\pi g9/2} \approx 1.0$. Furthermore, the γ-ray sequences on top of the $9/2^+$ states (^{61}Ga: 958-1039–1697 keV; ^{61}Zn: 937-1079–1675 keV) are very similar to the $6^+ \rightarrow 4^+ \rightarrow 2^+ \rightarrow 0^+$ ground-state cascade in the ^{60}Zn even-even "core" (1004-1189–1615 keV; see Fig. 1). Thus, it is not surprising that spectroscopic factors, C^2S, for $g_{9/2}$ proton emission from the corresponding excited states are calculated to be close to 1.0, e.g., $C^2S(9/2^+ \rightarrow 0^+) = 0.80$. Using the code Wspot [52] with standard parameters to estimate the single-particle decay width, Γ_{sp}, yields $\tau(9/2^+) = (\Gamma_{\mathrm{sp}} C^2S)^{-1} \approx 1$ fs. This is faster than any anticipated $E1$ or $M2$ electromagnetic decay of the $9/2^+$ state in ^{61}Ga (cf. Fig. 1).

In conclusion, a prompt 1.876(24)-MeV-proton-957.6(5)-keV-γ coincidence was detected in a unique multi-detector γ-ray spectroscopy experiment conducted at ANL. The discrimination of the proton-energy peak was made possible by implementing a novel particle-tracking DSSD system near the target position. The observed coincidence is associated with the γ-ray feeding of and proton emission from the proton $\pi g_{9/2}$ single-particle state at 2150(34) keV in the $N = Z - 1$ nucleus ^{61}Ga, populating the ground state of $N = Z$ ^{60}Zn. It is shown that shell-model calculations can reproduce the properties of quasibound states in ^{61}Ga and remain capable of describing MED even when states beyond the proton drip line are involved. Expanding the JUN45 shell-model interaction ($f_{5/2}pg_{9/2}$ space) with isospin-breaking terms provides a very good description of the measured MED in the $T_z = \pm 1/2$, $A = 61$ mirror pair. Future spectroscopy experiments beyond the proton drip line will help to consolidate the efforts for an improved theoretical description of $N \lesssim Z$ nuclei just above doubly magic ^{56}Ni, a region on the nuclear chart with considerable interest for nuclear astrophysics.

Acknowledgments—We thank the ATLAS accelerator crew for their supreme efforts. This research used resources of ANL's ATLAS facility, which is a DOE Office of Science User Facility. The isotopes used in this research were supplied by the U.S. Department of Energy Office of Science by the Isotope Program in the Office of Nuclear Physics. This research was funded in part by the Swedish Research Council (Vetenskapsrådet, VR 2016-3969, VR 2020-3721, and VR 2022-3828), the Crafoord Foundation in Lund (Grant No. 20180630), the U.S. Department of Energy, Office of Science, Office of Nuclear Physics (Contract No. DE-AC02-06CH11357), and the UKRI Science and Technology Facilities Council under Grants No. ST/P003885/1 and No. ST/V001035/1.

[1] M. A. Bentley and S. M. Lenzi, Prog. Part. Nucl. Phys. **59**, 497 (2007).
[2] J. Ekman, C. Fahlander, and D. Rudolph, Mod. Phys. Lett. A **20**, 2977 (2005).
[3] C. Langer *et al.*, Phys. Rev. Lett. **113**, 032502 (2014).
[4] D. Kahl *et al.*, Phys. Lett. B **797**, 134803 (2019).
[5] M. R. Bhat, Nucl. Data Sheets **85**, 415 (1998).
[6] C. Andreoiu, M. Axiotis, G. de Angelis, J. Ekman, C. Fahlander, E. Farnea, A. Gadea, T. Kröll, S. M. Lenzi, N. Mărginean, T. Martinez, M. N. Mineva, C. Rossi Alvarez, D. Rudolph, and C. A. Ur, Eur. Phys. J. A **15**, 459 (2002).
[7] L.-L. Andersson, E. K. Johansson, J. Ekman, D. Rudolph, R. du Rietz, C. Fahlander, C. J. Gross, P. A. Hausladen, D. C. Radford, and G. Hammond, Phys. Rev. C **71**, 011303 (R) (2005).
[8] R. Orlandi *et al.*, Phys. Rev. Lett. **103**, 052501 (2009).
[9] K. Wimmer *et al.*, Phys. Lett. B **847**, 138249 (2023).
[10] A. Fernández *et al.*, Phys. Lett. B **823**, 136784 (2021).
[11] R. D. O. Llewellyn *et al.*, Phys. Lett. B **811**, 135873 (2020).
[12] A. Obertelli, T. Baugher, D. Bazin, S. Boissinot, J.-P. Delaroche, A. Dijon, F. Flavigny, A. Gade, M. Girod, T. Glasmacher, G. F. Grinyer, W. Korten, J. Ljungvall, S. McDaniel, A. Ratkiewicz, B. Sulignano, P. Van Isacker, and D. Weisshaar, Phys. Lett. B **701**, 417 (2011).
[13] K. Zuber and B. Singh, Nucl. Data Sheets **125**, 1 (2015).
[14] L-L. Andersson, D. Rudolph, J. Ekman, C. Fahlander, E. K. Johansson, R. du Rietz, C. J. Gross, P. A. Hausladen, D. C. Radford, and G. Hammond, Eur. Phys. J. A **30**, 381 (2006).
[15] L.-L. Andersson, I. Ragnarsson, D. Rudolph, E. K. Johansson, D. A. Torres, C. Andreoiu, M. P. Carpenter, R. J. Charity, C. J. Chiara, J. Ekman, C. Fahlander, C. Hoel, O. L. Pechenaya, W. Reviol, R. du Rietz, D. G. Sarantites, D. Seweryniak, L. G. Sobotka, and S. Zhu, Phys. Rev. C **79**, 024312 (2009).
[16] N. Michel, W. Nazarewicz, and M. Płoszajczak, Phys. Rev. C **82**, 044315 (2010).
[17] E. Browne and J. K. Tuli, Nucl. Data Sheets **114**, 1849 (2013).

[18] Meng Wang, W. J. Huang, F. G. Kondev, G. Audi, and S. Naimi, Chin. Phys. C **45**, 030003 (2021).
[19] S. F. Paul *et al.*, Phys. Rev. C **104**, 065803 (2021).
[20] M. Wang *et al.*, Phys. Rev. Lett. **130**, 192501 (2023).
[21] See Supplemental Material at http://link.aps.org/supplemental/10.1103/kwm2-9bmd for more details.
[22] Y. Hrabar *et al.*, Acta Phys. Pol. B **18**, 2-A20 (2025).
[23] Y. Hrabar, Ph.D. thesis, Decay Modes of Exotic Nuclei, Lund University.
[24] D. G. Sarantites, P.-F. Hua, M. Devlin, L. G. Sobotka, J. Elson, J. T. Hood, D. R. LaFosse, J. E. Sarantites, and M. R. Maier, Nucl. Instrum. Methods Phys. Res., Sect. A **381**, 418 (1996).
[25] I.-Y. Lee, Nucl. Phys. **A520**, c641 (1990).
[26] D. G. Sarantites, W. Reviol, C. J. Chiara, R. J. Charity, L. G. Sobotka, M. Devlin, M. Furlotti, O. L. Pechenaya, J. Elson, P. Hausladen, S. Fischer D. Balamuth, and R. M. Clark, Nucl. Instrum. Methods Phys. Res., Sect. A **530**, 473 (2004).
[27] C. E. Svensson, J. A. Cameron, S. Flibotte, G. Gervais, D. S. Haslip, J. M. Nieminen, J. C. Waddington, J. N. Wilson, G. C. Ball, A. Galindo-Uribarri, V. P. Janzen, D. C. Radford, D. Ward, M. Cromaz, and T. E. Drake, Nucl. Instrum. Methods Phys. Res., Sect. A **396**, 228 (1997).
[28] C. N. Davids and J. D. Larson, Nucl. Instrum. Methods Phys. Res., Sect. B **40–41**, 1224 (1989).
[29] D. Rudolph, D. G. Sarantites, C. Andreoiu, C. Fahlander, D. P. Balamuth, R. J. Charity, M. Devlin, J. Eberth, A. Galindo-Uribarri, P. A. Hausladen, D. Seweryniak, L. G. Sobotka, and Th. Steinhardt, Eur. Phys. J. A **14**, 137 (2002).
[30] To our knowledge, this is the first time ever that particle-tracking-based beam-spot position corrections could be performed following fusion-evaporation reactions at large γ-ray detection arrays.
[31] D. Farghaly, M.Sc. thesis, Lund University, Sweden, 2022.
[32] M. B. L. Persson, B.Sc. thesis, Lund University, Sweden, 2022.
[33] J. F. Ziegler, Nucl. Instrum. Methods Phys. Res., Sect. B **219–220**, 1027 (2004).
[34] J. Allison, K. Amako, J. Apostolakis, P. Arce, M. Asai *et al.*, Nucl. Instrum. Methods Phys. Res., Sect. A **186**, 835 (2016).
[35] J. Allison, K. Amako, J. Apostolakis, H. Araujo, P. Arce Dubois *et al.*, IEEE Trans. Nucl. Sci. **53**, 270 (2006).
[36] S. Agostinelli, J. Allison, K. Amako, J. Apostolakis, H. Araujo *et al.*, Nucl. Instrum. Methods Phys. Res., Sect. A **506**, 250 (2003).
[37] E. K. Johansson, D. Rudolph, I. Ragnarsson, L.-L. Andersson, D. A. Torres, C. Andreoiu, C. Baktash, M. P. Carpenter, R. J. Charity, C. J. Chiara, J. Ekman, C. Fahlander, O. L. Pechenaya, W. Reviol, R. du Rietz, D. G. Sarantites, D. Seweryniak, L. G. Sobotka, C. H. Yu, and S. Zhu, Phys. Rev. C **80**, 014321 (2009).
[38] L.-L. Andersson *et al.*, Eur. Phys. J. A **36**, 251 (2008).
[39] This experiment was part of a campaign of five experiments aiming primarily at proton-unbound states in $N < Z$ nuclei beyond ^{56}Ni. The experiments were prepared late 2019 and early 2020 at ANL just prior to the outbreak of the Covid-19 pandemic. They were then run under severe restrictions at ANL during summer 2020 which allowed for only remote participation of non-ANL collaborators.
[40] D. Rudolph, D. Weisshaar, F. Cristancho, J. Eberth, C. Fahlander, O. Iordanov, S. Skoda, Ch. Teich, O. Thelen, and H. G. Thomas, Eur. Phys. J. A **6**, 377 (1999).
[41] E. Caurier, Shell model code Antoine, IRES, Strasbourg 1989–2002.
[42] E. Caurier and F. Nowacki, Acta Phys. Pol. **30**, 705 (1999), https://www.actaphys.uj.edu.pl/R/30/3/705.
[43] M. Honma, T. Otsuka, B. A. Brown, and T. Mizusaki, Phys. Rev. C **65**, 061301(R) (2002).
[44] D. Rudolph, C. Andreoiu, M. A. Bentley, M. P. Carpenter, R. J. Charity, R. M. Clark, J. Ekman, C. Fahlander, P. Fallon, W. Reviol, D. G. Sarantites, and D. Seweryniak, Phys. Rev. C **104**, 044314 (2021).
[45] D. Rudolph *et al.*, Phys. Lett. B **830**, 137144 (2022).
[46] M. Honma, T. Otsuka, T. Mizusaki, and M. Hjorth-Jensen, Phys. Rev. C **80**, 064323 (2009).
[47] A more comprehensive, full fp shell plus $g_{9/2}$, model space is to our knowledge not yet available for shell-model practitioners.
[48] The isospin-breaking JUN45 interaction file (for the Antoine shell-model code) used for this Letter can be made available upon request.
[49] J. Ekman, D. Rudolph, C. Fahlander, A. P. Zuker, M. A. Bentley, S. M. Lenzi, C. Andreoiu, M. Axiotis, G. de Angelis, E. Farnea, A. Gadea, T. Kröll, N. Mărginean, T. Martinez, M. N. Mineva, C. Rossi Alvarez, and C. A. Ur, Phys. Rev. Lett. **92**, 132502 (2004).
[50] S. M. Lenzi, M. A. Bentley, R. Lau, and C. Aa. Diget, Phys. Rev. C **98**, 054322 (2018).
[51] D. Rudolph, I. Ragnarsson, R. M. Clark, C. Andreoiu, M. P. Carpenter, J. Ekman, C. Fahlander, F. G. Kondev, T. Lauritsen, D. G. Sarantites, D. Seweryniak, and C. E. Svensson, Phys. Rev. C **103**, 034306 (2021).
[52] B. A. Brown and G. F. Bertsch, Woods Saxon Code for Bound States and Decay Widths (2011), https://people.nscl.msu.edu/~brown/reaction-codes.